

# SrTiO<sub>3</sub>–SrZrO<sub>3</sub> solid solution: Phase formation kinetics and mechanism through solid-oxide reaction

J. Bera<sup>a,\*</sup>, S.K. Rout<sup>b</sup>

<sup>a</sup>Department of Ceramic Engineering, National Institute of Technology, Rourkela 769008, India

<sup>b</sup>Department of Physics, National Institute of Technology, Rourkela 769008, India

---

## Abstract

The perovskite solid solution composition Sr(Ti<sub>0.5</sub>Zr<sub>0.5</sub>)O<sub>3</sub> (STZ (ss)) has been synthesized from the mixture of SrCO<sub>3</sub>, TiO<sub>2</sub> and ZrO<sub>2</sub> powders through solid-state reaction. The phase formation mechanism and kinetics were investigated using TG/DSC, XRD. SrCO<sub>3</sub> in the precursor decomposes at relatively lower temperature than pure powder decomposition, due to the presence of acidic TiO<sub>2</sub>. Upon calcinations of the precursor SrTiO<sub>3</sub> (ST) and SrZrO<sub>3</sub> (SZ) were formed separately in the system. Then ST diffuses in to SZ to form STZ (ss). ST formation started at lower temperature (800 °C) with lower activation energy (47.274 kcal/mol) than SZ. SZ formation started at 1000 °C with high activation energy (65.78 kcal/mol). STZ (ss) formation started from 1500 °C with very high activation energy (297.52 kcal/mol). It is concluded that solid solution formed coherently with SZ lattice by the diffusion of Ti in to the SZ.

*Keywords:* A. Ceramics; A. Electronic materials; A. Inorganic compounds; C. X-ray diffraction; D. Phase transactions

---

## 1. Introduction

Perovskite compounds are very attractive materials for practical use as well as academic research due to their variety of unique physical properties and rather simple structure. Different properties of perovskite like ferroelectric, magnetic, microwave, proton conduction, etc., can be combined and

---

\* Corresponding author. Tel.: +91 9437246159 (Mobile); fax: +91 6612462926.

*E-mail addresses:* jbera@nitrrkl.ac.in, jbera@rediffmail.com (J. Bera).

adjusted through their solid solution formation in a wide range of constituting cation with different size and charges. For example, the solid solutions; BaTiO<sub>3</sub>–SrTiO<sub>3</sub> and BaTiO<sub>3</sub>–SrZrO<sub>3</sub> are well established for multilayer capacitor composition [1,2] and PbZrO<sub>3</sub>–PbTiO<sub>3</sub> as piezoelectric ceramics [3]. In the last few years, perovskite solid solution, having super lattice structure had received great attention as a better proton conductor material [4]. SrTiO<sub>3</sub>–SrZrO<sub>3</sub> (ST–SZ) solid solution is one of them, which hold promise for application as a proton conductor as well as voltage dependent tunable ceramics [5]. ST–SZ solid solution shows a super lattice structure due to its cell enlargement as a result of tilting of BO<sub>6</sub> (B = Ti, Zr) octahedra [6]. This type of disorder perovskite solid solution offers exciting new possibilities both in the investigation of fundamental physical phenomena and in the exploitation of novel properties for various applications. There is very little literature [5–7] available for this solid solution system. In the present work, Sr(Ti<sub>0.5</sub>Zr<sub>0.5</sub>)O<sub>3</sub> solid solution (STZ (ss)) is synthesized through a solid oxide reaction route from the mixture of SrCO<sub>3</sub>, TiO<sub>2</sub> and ZrO<sub>2</sub>. The phase formation kinetics and solid solution formation mechanisms were investigated for the system.

## 2. Experimental

STZ-solid solutions were prepared by a solid-state reaction route from SrCO<sub>3</sub> (S.D. Fine Chem., Mumbai), TiO<sub>2</sub> (E. Merck India Ltd.) and ZrO<sub>2</sub> (Loba Chem., Mumbai). All the powders were of at least 99% purity. The particle size of starting raw materials, measured using Malvern Mastersizer, were: SrCO<sub>3</sub> [ $D(v,0.1) = 0.48 \mu\text{m}$ ,  $D(v,0.5) = 13.13 \mu\text{m}$ ,  $D(v,0.9) = 14.63 \mu\text{m}$ ], TiO<sub>2</sub> [ $D(v,0.1) = 0.27 \mu\text{m}$ ,  $D(v,0.5) = 0.35 \mu\text{m}$ ,  $D(v,0.9) = 0.48 \mu\text{m}$ ] and ZrO<sub>2</sub> [ $D(v,0.1) = 0.42 \mu\text{m}$ ,  $D(v,0.5) = 10.27 \mu\text{m}$ ,  $D(v,0.9) = 15.48 \mu\text{m}$ ]. The powders were thoroughly mixed in an agate mortar using propanol. The decomposition behavior of the raw mixture and pure SrCO<sub>3</sub> were investigated using a NETZSCH Thermal Analyzer. The mixed powder was calcined at different temperatures in the range 700–1600 °C for 1 h to study the phase formation behavior. The calcined powders were characterized with respect to phase identification, phase quantity measurement, crystallite size determination and lattice parameter measurement, etc., all by using Cu K $\alpha$  XRD (PW-1830, Philips, Netherlands). For quantitative estimation of phases, calcined powders were uniformly mixed with an internal standard and the resulting mixture was analyzed by XRD using a step size of 0.02°, 2 $\theta$  with 10 s/step. The relative weight fractions were quantified from the ratio of peak areas, according to the process described by Kumar and Messing [8]. On the basis of XRD line broadening at half maxima, crystallite sizes of the phases were estimated using the Scherrer equation [9].

## 3. Results and discussion

Fig. 1 shows a differential scanning calorimetric and thermo gravimetric (DSC-TG) tracing of the precursor. The TG graph shows a continuous weight loss from about 875–1100 °C. While the DSC graph shows two endothermic peaks at 928 and 1066 °C, respectively. The peak at 928 °C is due to the polymorphic transformation of SrCO<sub>3</sub> from the orthorhombic form (space group *Pmncn*) to the rhombohedral form (space group *R-3m*) [10]. The 1066 °C endothermic peak corresponds to the major decomposition reaction of SrCO<sub>3</sub> in the precursor. However, in pure SrCO<sub>3</sub> decomposition, that peak occurs at about 1130 °C. This indicates that SrCO<sub>3</sub> in the precursor reacts at relatively lower

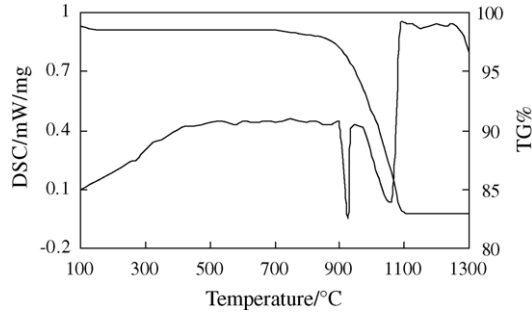


Fig. 1. TGA and DSC curve in air for the  $\text{SrCO}_3$ ,  $\text{TiO}_2$  and  $\text{ZrO}_2$  powder mixture.

temperature as per;  $\text{SrCO}_3 + \text{TiO}_2 = \text{SrTiO}_3 + \text{CO}_2$ , which is due to the presence of acidic  $\text{TiO}_2$  in the mixture [11].

Fig. 2 shows the XRD pattern of the precursor powder calcined at different temperatures for 1 h. It shows that ST and SZ form separately in the system and then STZ (ss) appears due to the inter-diffusion between ST and SZ. The 800 °C/1 h sample shows the presence of  $\text{SrTiO}_3$  in the calcined product. The  $\text{SrTiO}_3$  is formed due to the decomposition reaction of the precursor. The decomposition reaction releases

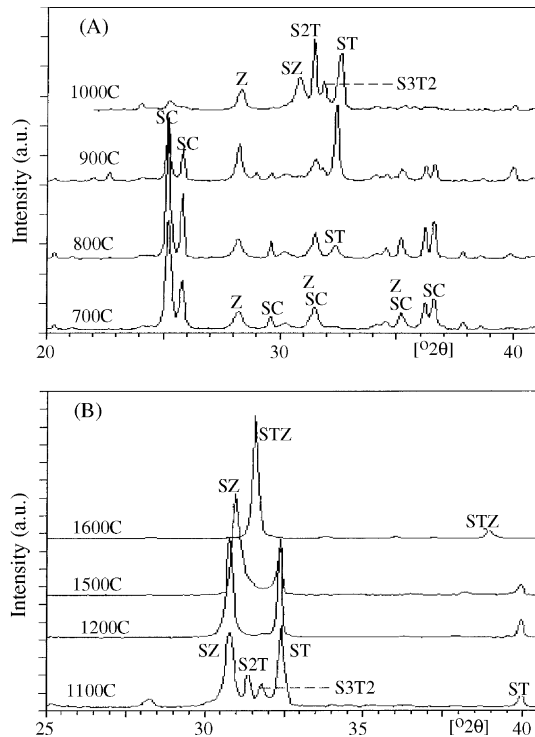


Fig. 2. XRD pattern of calcined precursor powder for 1 h at (A) 700, 800, 900 and 1000 °C and (B) at 1100, 1200, 1500 and 1600 °C; with notation: ST =  $\text{SrTiO}_3$ , SZ =  $\text{SrZrO}_3$ , S2T =  $\text{Sr}_2\text{TiO}_4$ , S3T2 =  $\text{Sr}_3\text{Ti}_2\text{O}_7$ , SC =  $\text{SrCO}_3$ , STZ (ss) =  $\text{Sr}(\text{Ti}_{0.5}\text{Zr}_{0.5})\text{O}_3$ , Z =  $\text{ZrO}_2$  and T =  $\text{TiO}_2$ .

highly reactive SrO in the system and that immediately reacts with TiO<sub>2</sub> to form ST. That may be the reason why SrO was not detected by XRD. The SZ phase was identified only from 1000 °C/1 h sample. Thus, the rate of formation of SZ was slower than ST in the system. That sample also shows the presence of two intermediate phases, Sr<sub>2</sub>TiO<sub>4</sub> and Sr<sub>3</sub>Ti<sub>2</sub>O<sub>7</sub> along with SrTiO<sub>3</sub>. The reason for the formation of Sr-rich intermediate phase may be due to the release of a huge amount of SrO in the system at that temperature range. At 1200 °C, Sr<sub>2</sub>TiO<sub>4</sub> and Sr<sub>3</sub>Ti<sub>2</sub>O<sub>7</sub> phases were not found due to their conversion into ST upon reacting with TiO<sub>2</sub> through Sr<sub>2</sub>TiO<sub>4</sub>-to-Sr<sub>3</sub>Ti<sub>2</sub>O<sub>7</sub>-to-SrTiO<sub>3</sub> and then only ST and SZ phases were found.

They start diffusing to form STZ (ss) in the temperature range 1300–1350 °C and STZ (ss) formation was complete in the range 1550–1600 °C. Intermediate phases like Sr<sub>2</sub>ZrO<sub>4</sub> were not observed within the detection limit of XRD. ST and SZ were found to match best with PDF no. 05-0634 for ST and 70-0283 for SZ, respectively. However, no standard pattern is available for Sr(Ti<sub>0.5</sub>Zr<sub>0.5</sub>)O<sub>3</sub> compound in PDF version-1998.

It is already indicated that the rate of SrZrO<sub>3</sub> formation is lower than that of SrTiO<sub>3</sub> formation. This may be due to the: (i) less acidic nature of ZrO<sub>2</sub> than that of TiO<sub>2</sub> and/or (ii) high average particle size of ZrO<sub>2</sub> (10.27 μm) than TiO<sub>2</sub> (0.35 μm) and/or (iii) higher ionic radius of Zr<sup>4+</sup> (0.72 Å) than that of Ti<sup>4+</sup> (0.61 Å). Variation of their phase content with calcination temperature is shown in Fig. 3. As 1300 °C/1 h sample shows maximum integrated intensities of ST and SZ phases, the quantities at that temperature were considered 100%. The quantity of ST apparently decreases at 1000 °C due to the conversion of some fraction of that to Sr<sub>2</sub>TiO<sub>4</sub> and Sr<sub>3</sub>Ti<sub>2</sub>O<sub>7</sub>. The quantity of ST is higher than that of SZ up to 1100 °C. After 1300 °C, quantities of two phases are decreased due to the conversion in to STZ (ss). But STZ (ss) was detectable only at 1500 °C through slow step scanning. After 1400 °C, quantity of ST decreases quicker than SZ, indicating ST easily diffuses into SZ to form STZ (ss). After 1500 °C, STZ (ss) increases rapidly.

To check the phase formation kinetics, concentrations of the phases were used to measure the activation energy for their formation using the following relationship, considering they follow the diminishing core model [12].

$$[1 - (1 - X_B)^{1/3}]^2 = \frac{2Kt}{R^2} \quad (1)$$

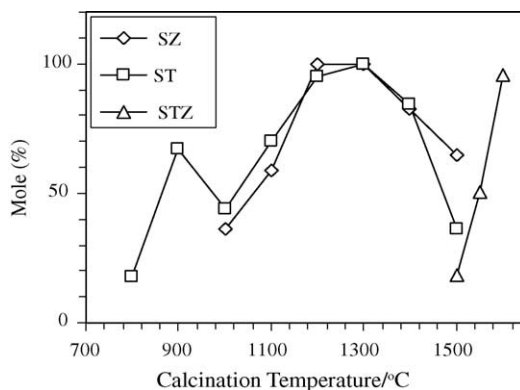


Fig. 3. Non-isothermal transformation kinetics of precursor in static air.

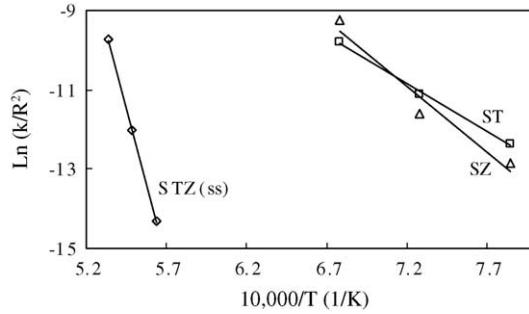


Fig. 4. Arrhenius dependence of reaction rate on calcination temperature for the formation of SrTiO<sub>3</sub> (□), SrZrO<sub>3</sub> (▲) and SrTi<sub>0.5</sub>Zr<sub>0.5</sub>O<sub>3</sub> solid solution (◇).

where  $2K/R^2$  is essentially a reaction rate constant,  $X_B$  the volume fraction reacted at time  $t$ .  $\text{Log}(K/R^2)$  versus  $1/T$  plot represents Arrhenius expression and activation energy for the phase formation can be derived from the slope of the plot.

Fig. 4 shows temperature dependency of their phase formation reactions. They show Arrhenius type of linear temperature dependency. The activation energy measured from the slope shows that ST formation requires less activation energy (47.27 kcal/mol) than that of SZ formation (65.78 kcal/mol) in the temperature range 1000–1300 °C. The activation energy found for SZ formation is in the same range of that found for BZ formation by Ubal dini et al. [13]. Phases were formed in this system through solid-state interdiffusion between different particles. Interdiffusions take place with different ions limiting the speed of diffusion. Activation energy results indicate that the phase formation reactions may be limited by the diffusion of Ti for ST and Zr for SZ formation, respectively. In the present case Sr and O are assumed to be immobile because their concentrations are spatially invariant, when compared for the two-perovskite structures. Since Zr<sup>4+</sup> has a larger ionic radius than Ti<sup>4+</sup>, its diffusion requires a higher energy than Ti<sup>4+</sup> to form perovskite phase.

STZ solid solution formation requires a much higher activation energy (297.52 kcal/mol). In the present case, a high activation energy found may be due to the use of loose powders for reaction kinetics experiment in compared to sintered pellets and/or use of un-doped material. For STZ (ss) formation, the rate of reaction may be limited by the diffusion of Ti through the SZ structure because the activation energy for the process is very similar to that calculated by Lewis et al. for the Ti-vacancy migration in BaTiO<sub>3</sub> [14].

The room temperature lattice parameters of the three phases present in the samples calcined at different temperatures are shown in Table 1 along with their x-ray crystallite size. These parameters of phases were calculated considering cubic structure for ST, orthorhombic for SZ and tetragonal for STZ (ss) as per Wong et al. [6]. For comparison only  $a_0$  values are given in Table 1. Lattice parameter of STZ (ss), found in the present study ( $a_0 = 5.6688(6)$  Å,  $c_0 = 8.0212$  Å) is similar to that reported ( $a_0 = 5.6650$  Å,  $c_0 = 8.011$  Å) by [6]. Previously we indicated that solid-solution formation takes place by the diffusion of ST into SZ lattices, as ST decomposes more rapidly than SZ. Also it is found that the lattice parameter of SZ decreases with increase in temperature from 1100 to 1400 °C (Table 1) due to the incorporation of smaller Ti<sup>4+</sup> ions in SZ. Whereas, lattice parameter of ST remains almost same up to 1400 °C, indicating there is negligible diffusion of Zr<sup>4+</sup> ion into ST structure. Some Zr<sup>4+</sup> ion diffusion into ST structure may be expected at higher temperature as 1500 °C samples shows slight

Table 1

Lattice parameter ' $a_0$ ' in Å and XRD-crystallite size in nm of ST, SZ and STZ (ss) in the samples calcined at different temperatures

Calcination temperature (°C)	SrTiO <sub>3</sub>		SrZrO <sub>3</sub>		STZ (ss)	
	$a_0$ (Å)	Crystallite size (nm)	$a_0$ (Å)	Crystallite size (nm)	$a_0$ (Å)	Crystallite size (nm)
800	3.9107(8)					
900	3.9054(8)					
1000	3.8957(9)	42.47	5.8004(9)	17.48		
1100	3.9039(7)	54.83	5.8037(9)	30.75		
1200	3.9076(5)	164.01	5.8048(9)	39.57		
1300	3.9037(6)	171.72	5.7967(8)	45.18		
1400	3.9083(3)	217.31	5.7899(6)	53.37		
1500	3.9126(2)	411.57	5.7753(5)	67.39	5.6882(9)	14.49
1550	–		–		5.6755(9)	45.55
1600	–		–		5.6715(8)	59.0
1650	–		–		5.6688(6)	65.0

increase in ' $a_0$ ' value of ST. Table 1 also shows that STZ (ss) has higher lattice parameter at 1500 °C than that at 1600 °C, indicating initial solid solution is higher in Zr<sup>4+</sup> ion content than the final equilibrium one. Thus, it may be considered that solid solution forms on SZ lattices having a coherent interface with SZ crystal, but not on the ST lattice. The XRD peaks of STZ (ss) which forms between [1 1 0] peak of ST and [2 0 0] peak of SZ (Fig. 2b) was indexed as overlapping [0 2 0], [1 1 2] reflections of tetragonal STZ (ss) phase. If solid solution forms on ST lattice, one would expect that peak be composed of [1 1 0], [1 0 1] reflections of tetragonal structure. But the present investigation shows the peak was for [0 2 0] reflection of tetragonal structure. That indicates that the solid solution is formed coherently with [2 0 0] plane of SZ. A similar coherent interface between BaZrO<sub>3</sub> and Ba(Ti<sub>0.6</sub>Zr<sub>0.4</sub>)O<sub>3</sub> lattices was also found by the authors [15]. This mechanism also suggests that the morphology of STZ (ss) should be controlled by the morphology of SZ phase formed in the intermediate stage. Table 1 also shows the XRD crystallite sizes of SZ, ST and STZ (ss) at different temperatures. Crystallite size of ST is always much higher than SZ, which again indicates the easy formation of ST in the system.

#### 4. Conclusions

Sr(Ti<sub>0.5</sub>Zr<sub>0.5</sub>)O<sub>3</sub> solid solution was formed through solid-state reaction from a mixture of SrCO<sub>3</sub>, TiO<sub>2</sub> and ZrO<sub>2</sub>, via the formation of SrTiO<sub>3</sub> and SrZrO<sub>3</sub> phases separately in the system and then inter-diffusion of SrTiO<sub>3</sub> into SrZrO<sub>3</sub> to form the solid solution.

The rate of SrTiO<sub>3</sub> formation was higher than SrZrO<sub>3</sub> formation, apparently due to the higher ionic radius of Zr<sup>4+</sup> ions. The activation energy of the phase formations were 47.27, 65.78 and 297.52 kcal/mol for SrTiO<sub>3</sub>, SrZrO<sub>3</sub> and Sr(Ti<sub>0.5</sub>Zr<sub>0.5</sub>)O<sub>3</sub>, respectively, and the formation reactions were limited by the diffusion of Sr ion for SrTiO<sub>3</sub>, Zr ion for SrZrO<sub>3</sub> and Ti ions for Sr(Ti<sub>0.5</sub>Zr<sub>0.5</sub>)O<sub>3</sub>, etc. The solid solution was formed coherently with the crystal of SrZrO<sub>3</sub>.

## References

- [1] J. Daniels, K.H. Hardl, R. Wernicke, *Philips Tech. Rev.* 38 (1978) 73–82.
- [2] J. Gerblinger, H. Meixner, *Sens. Actuators B4* (1991) 99–102.
- [3] B. Jaffe, W.R. Cook Jr., H. Jaffe, *Piezoelectric Ceramics*, Academic Press, New York, 1971, pp. 1–5.
- [4] H. Yugami, F. Iguchi, H. Naito, *Solid State Ionics* 136–137 (2000) 203–207.
- [5] H.M. Christen, L.A. Knauss, K.S. Harshvardhan, *Mater. Sci. Eng. B56* (1998) 200–203.
- [6] T.K.Y. Wong, B.J. Kennedy, C.J. Howard, B.A. Hunter, T. Vogt, *J. Solid State Chem.* 156 (2001) 255–263.
- [7] F. Ernst, A. Recnik, P.A. Langjahr, P.D. Nellist, M. Ruhle, *Acta Mater.* 47 (1) (1998) 183–198.
- [8] S. Kumar, G.L. Messing, *J. Am. Ceram. Soc.* 77 (11) (1994) 2940.
- [9] H.P. Klug, L.E. Alexander, *X-ray Diffraction Procedures*, Wiley, New York, 1954, p. 491.
- [10] R.C. Evans, *An Introduction to Crystal Chemistry*, Cambridge University Press, Cambridge, UK, 1966, p. 410.
- [11] M. Stockenhuber, H. Mayer, J.A. Lercher, *J. Am. Ceram. Soc.* 76 (5) (1993) 1185.
- [12] T.A. Ring, *Fundamentals of Ceramic Powder Processing and Synthesis*, Academic Press Inc., 1996, p. 174.
- [13] A. Ubaldini, V. Buscaglia, C. Uliana, G. Costa, M. Ferretti, *J. Am. Ceram. Soc.* 86 (1) (2003) 19–25.
- [14] G.V. Lewis, C.R.A. Catlow, *Radiat. Eff.* 73 (1983) 307–314.
- [15] J. Bera, S.K. Rout, *Mater. Lett.* 59 (1) (2005) 135–138.